

# Process Intensification on the Separation of Benzene and Thiophene by Extractive Distillation

Jingli Han, Zhigang Lei, Yichun Dong, Chengna Dai, and Biaohua Chen

State Key Laboratory of Chemical Resource Engineering, Beijing University of Chemical Technology, Box 266, Beijing 100029, China

DOI 10.1002/aic.15009

Published online August 22, 2015 in Wiley Online Library (wileyonlinelibrary.com)

*The separation of benzene and trace thiophene by extractive distillation was intensified in two aspects, that is, selection of a suitable entrainer and improvement of the process. The mixture of dimethylformamide (DMF) and an ionic liquid (IL) was chosen as the entrainer. Vapor–liquid equilibrium (VLE) experiments using pure DMF and a mixed entrainer were conducted, and UNIFAC model for ILs was extended to the benzene–thiophene–DMF–IL system. The results demonstrated that volatilization loss of DMF in the vapor phase was significantly reduced by adding IL. Moreover, an improved process with only four columns using a mixed entrainer was proposed. The results indicated that the improved process is more promising for decreasing energy consumption and equipment investment compared with the conventional six-column process. The total heat duties of reboilers and condensers was decreased by 6.47% and 6.41%, respectively. The process intensification strategy may be directly extended to separate trace components of other systems. © 2015 American Institute of Chemical Engineers AICHE J, 61: 4470–4480, 2015*

**Keywords:** extractive distillation, benzene, thiophene, ionic liquids, UNIFAC model, process intensification

## Introduction

Benzene is a precursor to heavy chemicals, such as ethylbenzene and cumene. As a common contaminant in benzene, thiophene harms benzene process industry, for example, eroding metallic equipment, making catalyst poisoning, affecting products quality, and causing environmental pollution. There is an urgent need to remove thiophene to ensure the high purity of benzene. Therefore, separation of the benzene–thiophene mixture is of great industrial interest in purification technology. The separation of azeotropic or close boiling binary mixtures is very difficult using ordinary distillation processes. As a result, extractive distillation, a special distillation technique that removes certain compounds from close-boiling mixtures in industrial processes, has received much attention.<sup>1–12</sup>

Selection of suitable solvents and design of extractive distillation processes are two key factors for saving energy and decreasing emissions.<sup>13–16</sup> Dimethylformamide (DMF) is a common and suitable organic solvent for separating mixtures of benzene and thiophene. In recent years, many researchers have been engaged in improving and optimizing conventional solvents<sup>17–23</sup> because of their ubiquitous disadvantages (i.e., large solvent usage, high energy consumption, and low plate efficiency). Ionic liquids (ILs) have been widely used as entrainers in extractive distillation<sup>24–34</sup> due to their negligible vapor pressure, nonflammability, thermal stability, and high

selectivity for both polar and nonpolar compounds. However, when a pure IL is used as an entrainer, miscibility with nonpolar compounds is a significant problem during actual operation in addition to its high price. Thus, in this work, the mixture of an organic solvent (DMF) and an IL is proposed as an entrainer for the separation of benzene and thiophene to reduce the content of DMF in product stream. Herein, the IL [EMIM][BF<sub>4</sub>] was selected because it has a small molecular structure and a sterical shielding effect around the anion charge center, which are favorable properties for separation of nonpolar systems.<sup>18</sup> Moreover, [EMIM][BF<sub>4</sub>] can be bought from chemical markets at a relatively low price and possesses the advantages of low viscosity (45.1 mPa·s at 298.2 K) and good thermal stability. It should be noted that addition of the IL did not alter the flow sheet or increase the equipment cost. Furthermore, process miniaturization is another key factor for economic design of extractive distillation processes. To minimize the equipment investment, the conventional six-column extractive distillation process for this separation should be simplified.

It is important to select an efficient thermodynamic model for process simulation. Activity coefficient models (e.g., Wilson, NRTL, UNIQUAC, and UNIFAC) are commonly used to describe phase equilibrium of systems containing ILs due to their solid thermodynamic foundation and fast calculation speed. UNIFAC model is a functional group-contribution model that assumes the interaction energy between particular groups is constant regardless of the overall structures of the components. Thus, the model can be easily extended to other systems with similar groups. For instance, the interaction parameters for DMF and thiophene obtained in this work can be directly applied to systems containing DMF and other

Additional Supporting Information may be found in the online version of this article.

Correspondence concerning this article should be addressed to Z. Lei at leizhg@mail.buct.edu.cn.

thiophene-type sulfides (e.g., methylthiophene, ethylthiophene, benzothiophene, and dibenzothiophene).

The aim of this work was to intensify the extractive distillation process by altering the entrainer and process flow sheet for separation of benzene and thiophene. The remainder of this article is organized into the following three sections. First, vapor–liquid equilibrium (VLE) data for the benzene and thiophene system were measured at atmospheric pressure (101.3 kPa) using pure DMF and the DMF + [EMIM][BF<sub>4</sub>] mixture as an entrainer. Second, the UNIFAC model for ILs was established based on the obtained VLE experimental data. The corresponding model parameters were derived and input into the process simulation software. Finally, an improved extractive distillation process was proposed, and the separation performance was compared with that of the conventional six-column process.

## Experimental Section

### Materials

The experimental materials used in this work were benzene, thiophene, DMF, and the IL [EMIM][BF<sub>4</sub>]. Benzene with a purity above 99.5 wt % was obtained from Tianjin Guangfu Fine Chemical Research Institute. Thiophene and DMF with purities above 99 wt % and 99.9 wt %, respectively, were supplied by Beijing J&K Scientific. The IL [EMIM][BF<sub>4</sub>] with a purity above 99.5 wt % was purchased from Shanghai ChengJie Chemical Co. Prior to an experiment, the IL was purified to remove traces of water and volatile impurities using a vacuum rotary evaporator at 333.2 K for 12 h. The water content was controlled to be less than 400 ppm after drying. The other chemicals were used without further treatment.

### Apparatus and procedure

The VLE data were measured using a circulation VLE still at atmospheric pressure. A detailed description of the VLE still is available in our previous publications.<sup>35–37</sup> The compositions of benzene, thiophene, DMF, and [EMIM][BF<sub>4</sub>] in the liquid and vapor phases were analyzed by a gas chromatograph (GC 4000A) using a flame ionization detector (FID) and an HJ-WAX column (60 m × 0.32 mm). Data analysis was performed using an SC1100 workstation, and the compositions of the mixtures were calculated using the peak areas of the samples.

## Computational Details

### The UNIFAC model for ILs

The UNIFAC model for ILs, which is based on the group contribution method, was used to predict the thermodynamic behavior of the systems containing benzene, thiophene, and the IL. There are three main methods for dividing one IL molecule into several separate functional groups. (1) The IL molecule can be divided into one cation group and one anion group.<sup>38,39</sup> Evidently, this method does not reflect the influence of structural variation of substituents of the cations (or anions) on the thermodynamic properties. (2) The IL molecule can be divided into several groups with the imidazolium or pyrrolidinium ring as a functional group.<sup>40–45</sup> Although the structural variations of cations, anions, and substituents are adequately considered in this method, a large number of experimental data are required to correlate the group interaction parameters. Therefore, only a few IL functional groups have been included because experimental data available in the literature were limited. (3) The structures of cations and anions of ILs can be treated as a whole group because the ionic pair

has a strong electrostatic interaction.<sup>46–48</sup> For example, [EMIM][BF<sub>4</sub>] can be divided into one CH<sub>3</sub> group, one CH<sub>2</sub> group, and one [MIM][BF<sub>4</sub>] group. In this work, the last method was adopted to avoid additional terms accounting for long electrostatic contributions. The benzene molecule was divided into six ACH groups, whereas thiophene and DMF were treated as one separate group.

The activity coefficient  $\gamma_i$  can be calculated as follows

$$\ln \gamma_i = \ln \gamma_i^C + \ln \gamma_i^R \quad (1)$$

where  $\ln \gamma_i^C$  represents the combinatorial contribution to the activity coefficient due to differences in the sizes and shapes of the groups, and  $\ln \gamma_i^R$  represents the residual contribution from energetic interactions.

$\ln \gamma_i^C$  contains the group parameters  $R_k$  and  $Q_k$  and can be derived as follows

$$\ln \gamma_i^C = 1 - V_i + \ln V_i - 5q_i \left( 1 - \frac{V_i}{F_i} + \ln \left( \frac{V_i}{F_i} \right) \right) \quad (2)$$

$$F_i = \frac{q_i}{\sum_j q_j x_j}; V_i = \frac{r_i}{\sum_j r_j x_j} \quad (3)$$

$$r_i = \sum_k v_k^{(i)} R_k; q_i = \sum_k v_k^{(i)} Q_k \quad (4)$$

$$R_k = \frac{V_k \times N_A}{V_{VW}}, Q_k = \frac{A_k \times N_A}{A_{VW}} \quad (5)$$

where  $v_k^{(i)}$  is the number of group  $k$  in molecule  $i$ ;  $V_k$  and  $A_k$  are the group volume and surface area, respectively;  $V_{VW}$  (15.17 cm<sup>3</sup> mol<sup>−1</sup>) and  $A_{VW}$  (2.5 × 10<sup>9</sup> cm<sup>2</sup> mol<sup>−1</sup>) are the standard segment volume and surface area, as suggested by Bondi,<sup>49</sup> respectively; and  $N_A$  is Avogadro's number (6.023 × 10<sup>23</sup> mol<sup>−1</sup>). The parameters  $R_k$  and  $Q_k$  for the groups investigated in this work can be found in the literature.<sup>48,50</sup>

$\ln \gamma_i^R$  is a function of binary interaction parameters between groups, as follows

$$\ln \gamma_i^R = \sum_k v_k^{(i)} [\ln \Gamma_k - \ln \Gamma_k^{(i)}] \quad (6)$$

$$\ln \Gamma_k = Q_k \left[ 1 - \ln \left( \sum_m \theta_m \psi_{mk} \right) - \sum_m \left( \theta_m \psi_{km} / \sum_n \theta_n \psi_{nm} \right) \right] \quad (7)$$

$$\theta_m = \frac{Q_m X_m}{\sum_n Q_n X_n}; X_m = \frac{\sum_i v_m^{(i)} x_i}{\sum_i \sum_k v_k^{(i)} x_i} \quad (8)$$

where  $\Gamma_k$  is the group residual activity coefficient;  $\Gamma_k^{(i)}$  is the residual activity coefficient of group  $k$  in a reference solution containing only molecules of type  $i$ ; and  $X_m$  is the fraction of group  $m$  in the mixture. The group interaction parameter  $\psi_{nm}$  is expressed as follows

$$\psi_{nm} = \exp[-(\alpha_{nm}/T)] \quad (9)$$

where  $T$  is the absolute temperature,  $\alpha_{nm}$  is the temperature-independent parameter for each pair of functional groups  $n$  and  $m$ , and  $\alpha_{nm} \neq \alpha_{mn}$ .

The group binary interaction parameters were obtained by correlating the equilibrium experimental data. The following minimized objective function ( $OF$ ) was used to obtain the group interaction parameters

**Table 1. The Group Interaction Parameters of Benzene, Thiophene, IL, and DMF for the UNIFAC Model**

<i>m</i>	<i>n</i>	$\alpha_{mn}$	$\alpha_{nm}$
ACH	Thiophene	−39.16	23.93
ACH	DMF	245.6	−133.9
ACH	CH <sub>2</sub>	−11.12	61.13
ACH	[MIM][BF <sub>4</sub> ]	1494.39	85.64
Thiophene	CH <sub>2</sub>	−8.479	92.99
DMF	CH <sub>2</sub>	−31.95	485.3
CH <sub>2</sub>	[MIM][BF <sub>4</sub> ]	1108.51	588.74
Thiophene	DMF	396.39 <sup>a</sup>	−235.62 <sup>a</sup>
Thiophene	[MIM][BF <sub>4</sub> ]	676.31	−42.93
DMF	[MIM][BF <sub>4</sub> ]	−495.82 <sup>a</sup>	−263.92 <sup>a</sup>

<sup>a</sup>Group binary interaction parameters obtained in this work; others are from references.<sup>48,50,59</sup>

$$OF = \min \left\{ \frac{1}{N} \sum_{i=1}^N \left| \frac{\gamma_{i,\text{cal}} - \gamma_{i,\text{exp}}}{\gamma_{i,\text{exp}}} \right| \right\} \quad (10)$$

where  $\gamma_{i,\text{exp}}$  and  $\gamma_{i,\text{cal}}$  are the activity coefficients of component *i* in the liquid phase obtained from the experimental data and by the UNIFAC model, respectively; and *N* is the number of data points. During the correlation process, the activity coefficients of both benzene and thiophene were included. The Marquardt method, as described in Press et al.,<sup>51</sup> was used to fit the parameters  $\alpha_{nm}$  and  $\alpha_{mn}$ . The fitting procedure was performed in a similar manner as in our previous publication.<sup>48</sup>

Thus, the group parameters of DMF/thiophene and DMF/IL were obtained using the VLE data of the quaternary system. All of the group interaction parameters,  $\alpha_{nm}$  and  $\alpha_{mn}$ , used in this work are listed in Table 1, and the current UNIFAC parameter matrix for ILs is illustrated in Figure 1.

### Process simulation

The conventional and improved extractive distillation processes were simulated using Aspen Plus software (version 7.2) with the rigorous equilibrium (EQ) stage model RadFrac.<sup>60–63</sup> The UNIFAC model was selected, and the new model param-

eters obtained in this work were input into the software. In process simulation, benzene, thiophene and DMF were considered conventional compounds from the Aspen Plus database. The IL was defined as a new component by the “User Defined” function<sup>64–66</sup> and its critical properties were estimated by group contribution methods.<sup>38,39,44</sup>

## Results and Discussion

### Relative volatility of benzene to thiophene with [EMIM][BF<sub>4</sub>] as an entrainer and an liquid–liquid equilibrium diagram

The VLE data for the binary system of benzene (1) + thiophene (2) were first measured, and the results are presented in Table S1 in the Supporting Information. In Table S1,  $p_i^s$  represents the vapor pressure of pure component *i* and was obtained using the Antoine equation. The Antoine equation parameters are given in Table S2 in the Supporting Information. The thermodynamic consistency test results showed that the binary VLE data were thermodynamically consistent (more details can be found in Figure S1 in the Supporting Information). The relative volatility ( $\alpha_{12}$ ) of benzene (1) to thiophene (2) was calculated as follows

$$\alpha_{12} = \frac{y_1/x_1}{y_2/x_2} \quad (11)$$

The relative volatility of benzene (1) to thiophene (2) using [EMIM][BF<sub>4</sub>] as an entrainer is presented in Figure 2a, and the detailed experimental data are listed in Table S3 in the Supporting Information. As the IL concentration was increased, the relative volatility of benzene to thiophene first increased, then decreased after undergoing a local extreme point, and finally increased again. Thus, one “relative volatility peak” (or “separation factor peak”) appeared in the experimental concentration range, which conforms to a previous report regarding the separation of *n*-hexane and 1-hexene with ILs.<sup>18</sup> When the addition of IL was greater than the value corresponding to the relative volatility peak, formation of the

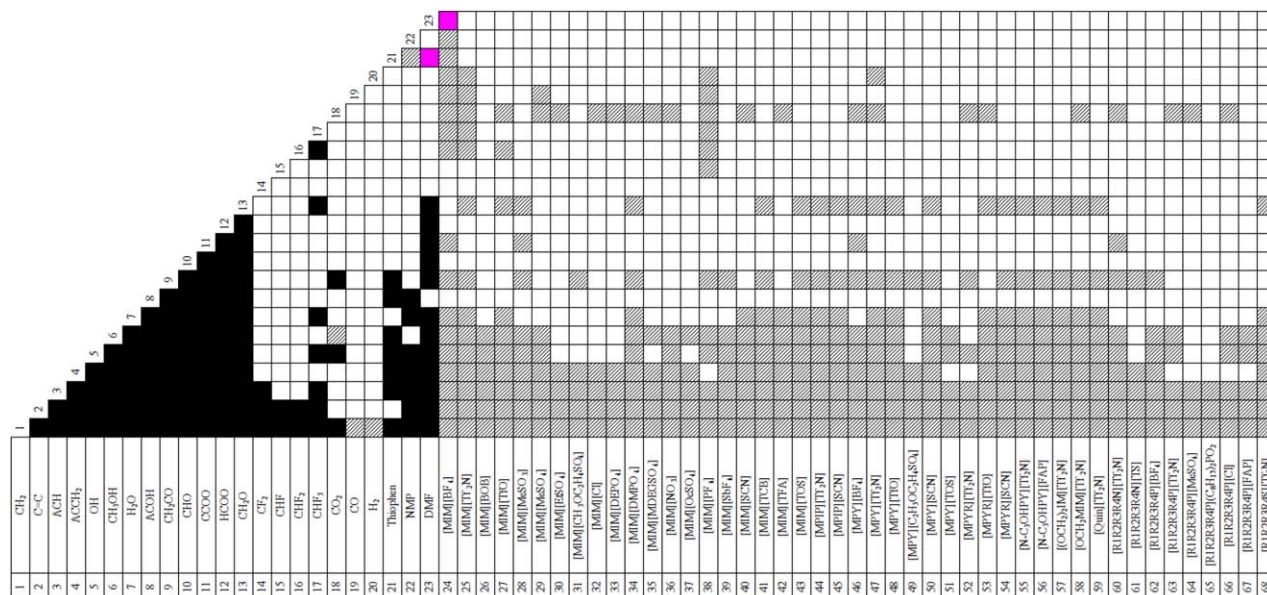


**Figure 1. Current UNIFAC parameter matrix for ILs.**

(■) Previously published parameters<sup>50,52–55</sup>; (■) Previously published parameters by our group<sup>48,56–59</sup>; (■) New parameters (this work); (□) No parameters available. [Color figure can be viewed in the online issue, which is available at [www.interscience.wiley.com](http://www.interscience.wiley.com).]



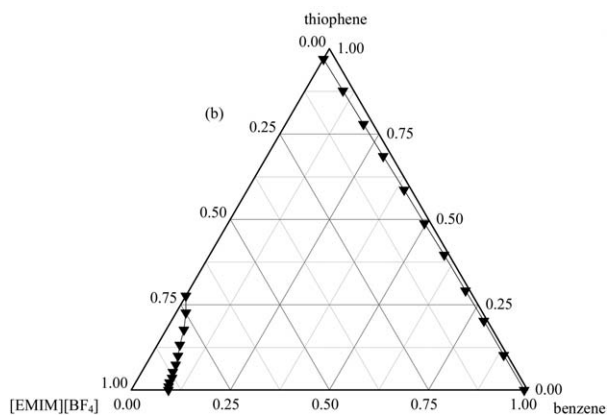
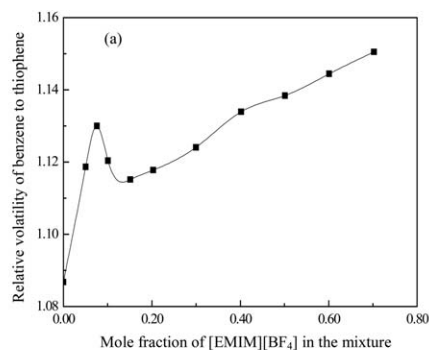


**Figure 2.** Relative volatility of benzene (1) to thiophene (2) using [EMIM][BF<sub>4</sub>] as an entrainer (a) and the LLE diagram at 343.2 K (b).

second liquid was observed visually. In this case, the IL mainly remained in the lower IL phase, which could not exert its effect on the upper organic phase, and, thus, the relative volatility was decreased slightly. According to the common parameter of “like dissolves like,” this separation phenomenon may be related to the formed liquid–liquid phase demixing during the VLE.

To further investigate the effect of phase demixing on separation performance, liquid–liquid equilibrium (LLE) experiments of benzene, thiophene, and [EMIM][BF<sub>4</sub>] ternary systems were conducted at 343.2 K using the cloud-point method, and the results are shown in Figure 2b. As seen, the second liquid phase was formed, and the IL could not exert its separation ability for the upper organic phase but mostly remained in the lower IL phase. Thus, liquid–liquid phase demixing was unfavorable for separation. Benzene and thiophene were found to be partly miscible with [EMIM][BF<sub>4</sub>] but completely miscible with DMF at the boiling temperature. Therefore, the combination of [EMIM][BF<sub>4</sub>] and DMF not only ensured the high solubility of the mixed entrainer with benzene or thiophene but also maintained the strong separation capability of the IL.

#### Relative volatility using pure DMF and the mixture of DMF + IL as entrainers

The VLE data for the benzene (1) + thiophene (2) + DMF (3) ternary and the benzene (1) + thiophene (2) + DMF (3) + [EMIM][BF<sub>4</sub>] (4) quaternary systems are listed in Tables S4 and S5 in the Supporting Information, respectively.

The  $y'_1-x'_1$  (on an entrainer-free basis) profiles using the DMF and IL as a mixed entrainer (mass fraction of IL in mixed the entrainer was kept at 10 wt % and 20 wt %) as well

as the benchmarked solvent DMF in a full concentration range are shown in Figure 3, along with the results predicted by the UNIFAC model. The predicted results and experimental data

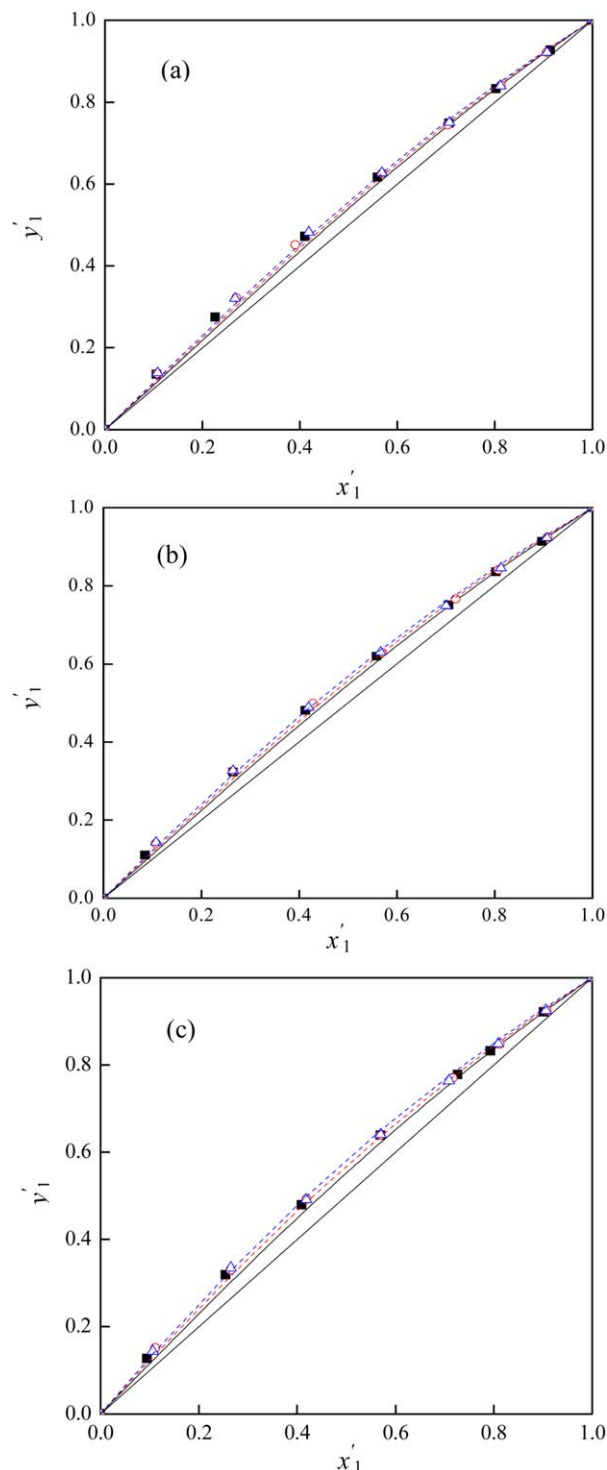


**Figure 3.** Isobaric VLE data for the benzene (1) + thiophene (2) system at 101.3 kPa using the mixed entrainer [DMF (3) + [EMIM][BF<sub>4</sub>] (4)].

(a)  $x_{\text{entrainer}} = 20\%$ ; (b)  $x_{\text{entrainer}} = 30\%$ ; (c)  $x_{\text{entrainer}} = 40\%$ . Lines, data predicted by the UNIFAC model; scattered points, experimental data. (■)  $w_4 = 0\%$ ; (○)  $w_4 = 10\%$ ; (△)  $w_4 = 20\%$ . [Color figure can be viewed in the online issue, which is available at [wileyonlinelibrary.com](http://wileyonlinelibrary.com).]

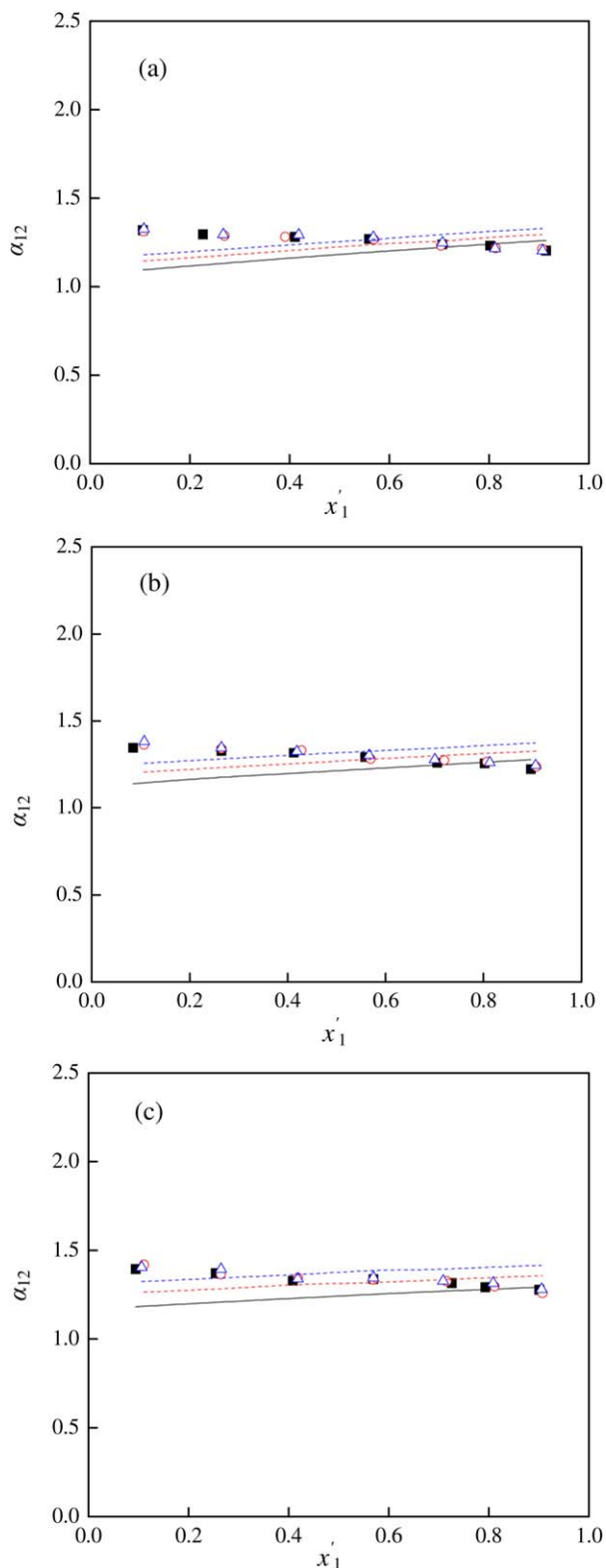


**Figure 4.** Relative volatility of benzene (1) to thiophene (2) using the mixed entrainer (DMF + [EMIM][BF<sub>4</sub>]).

(a)  $x_{\text{entrainer}} = 20\%$ ; (b)  $x_{\text{entrainer}} = 30\%$ ; (c)  $x_{\text{entrainer}} = 40\%$ . Lines, predicted data by the UNIFAC model; scattered points, experimental data. (■)  $w_4 = 0$ ; (●)  $w_4 = 10\%$ ; (▲)  $w_4 = 20\%$ . [Color figure can be viewed in the online issue, which is available at [wileyonlinelibrary.com](http://wileyonlinelibrary.com).]

agree well, and the ARDs for the ternary and quaternary systems were 4.02% and 2.89%, respectively, confirming that the UNIFAC model for ILs developed by us is reliable and accurate. Thus, the new UNIFAC interaction parameters can be

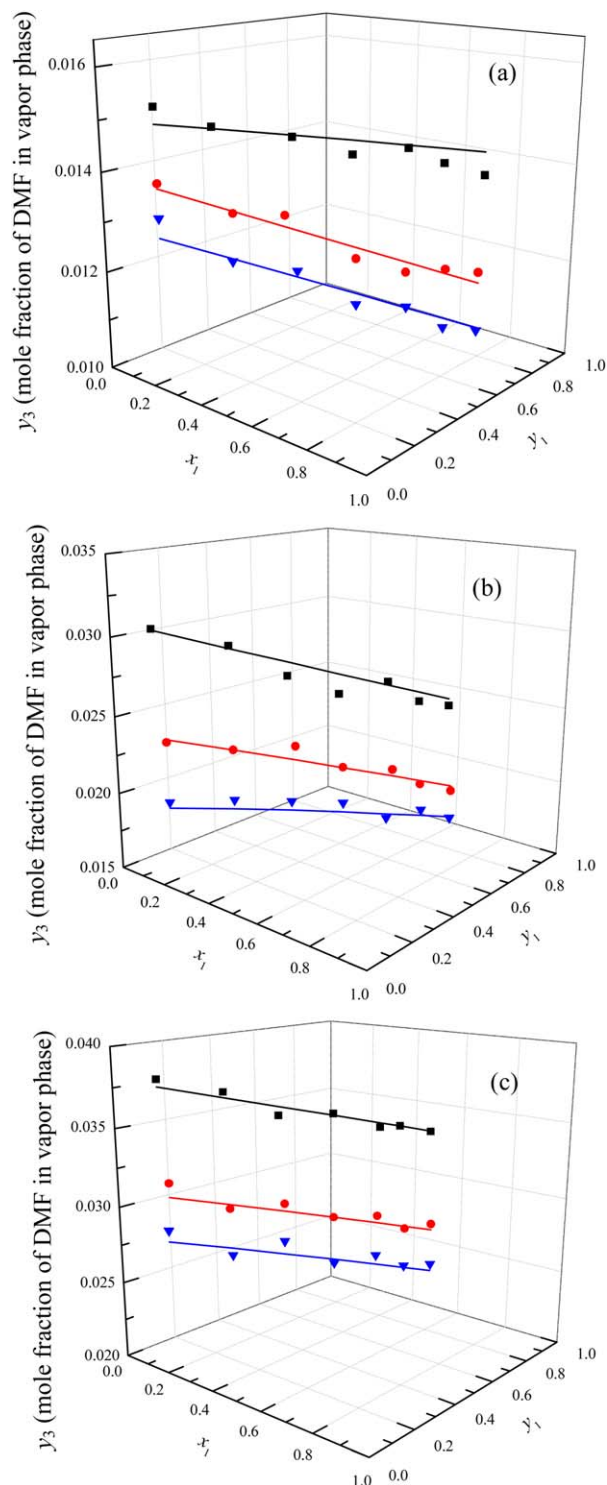


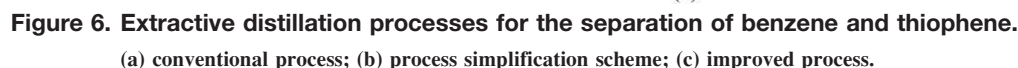
**Figure 5.** The DMF content in the vapor phase for benzene (1) + thiophene (2) + the mixed entrainer [DMF (3) + [EMIM][BF<sub>4</sub>] (4)] system at 101.3 kPa.

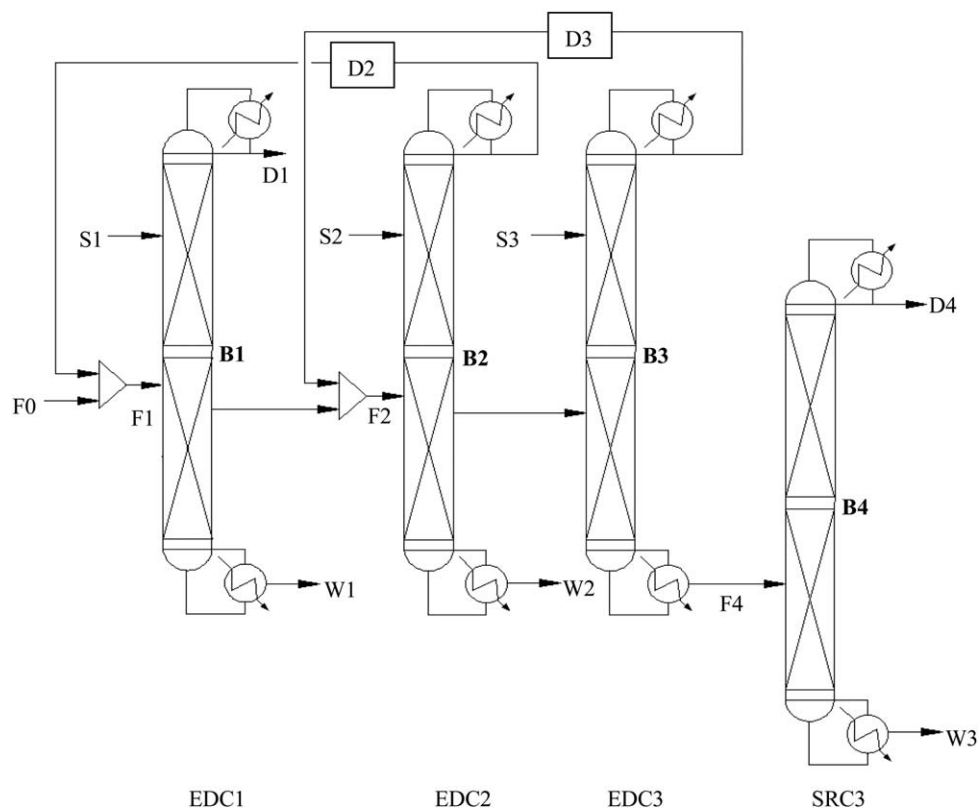
(a)  $x_{\text{entrainer}} = 20\%$ ; (b)  $x_{\text{entrainer}} = 30\%$ ; (c)  $x_{\text{entrainer}} = 40\%$ . (■)  $w_4 = 0$ ; (●)  $w_4 = 10\%$ ; (▼)  $w_4 = 20\%$ . [Color figure can be viewed in the online issue, which is available at [wileyonlinelibrary.com](http://wileyonlinelibrary.com).]

The profiles of relative volatility  $\alpha_{12}$  along  $x'_1$  are shown in Figure 4. As seen, the increase in relative volatility was not

### Volatilization loss of DMF in the vapor phase

The volatilization loss of DMF in the vapor phase was further studied in this work, and the results are presented in





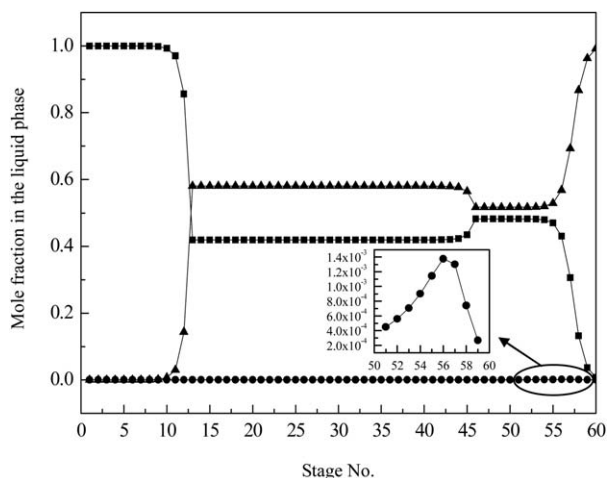
(c)  
Figure 6. (Continued).

Figure 5. As seen, the mole fraction of DMF in the vapor phase ( $y_3$ ) was significantly reduced when using the mixed entrainer compared with pure DMF. This was attributed to the following two reasons: (1) the amount of DMF in the mixed entrainer was less than that in the pure DMF entrainer, and (2) the interaction between DMF and IL caused less DMF to vola-

tilize into the vapor phase. Therefore, the benzene product obtained at the top of the extractive distillation column can be further purified when using the mixture of DMF and [EMIM][BF<sub>4</sub>] as an entrainer for the separation of benzene and thiophene. This step is especially important to obtain the high-purity benzene product with impurity content of less than

Table 2. Operating Conditions and Optimized Specifications for Conventional and Improved Extractive Distillation Processes

Contents		Conventional process	Improved process	Contents		Conventional process	Improved process	
EDC1	Pressure (atm)	1	1	SRC1	Pressure (atm)	1	—	
	Total stage	60	60		Total stage	60	—	
	Feed (F1) stage	46	46		Feed stage	11	—	
	Solvent (S1) feed stage	13	13		Mass reflux ratio	28.7	—	
	Mass reflux ratio	5.6	6.3		Distillate rate (kg h <sup>-1</sup> )	50	—	
	Distillate rate D1 (kg h <sup>-1</sup> )	950	950		SRC2	Pressure (atm)	1	—
	Side-stream (Side 1) stage	—	56			Total stage	60	—
	Side-stream (Side 1) mass flow rate (kg h <sup>-1</sup> )	—	1700			Feed stage	11	—
EDC2	Pressure (atm)	1	1	SRC3	Mass reflux ratio	15.9	—	
	Total stage	60	60		Distillate rate (kg h <sup>-1</sup> )	3.02	—	
	Feed (F2) stage	46	37		Pressure (atm)	1	1	
	Solvent (S2) feed stage	10	8		Total stage	60	60	
	Mass reflux ratio	3.1	9.4		Feed stage	44	42	
	Distillate rate D2 (kg h <sup>-1</sup> )	49.4	49.4		Mass reflux ratio	13.1	75	
	Side-stream (F3) stage	—	38		Entrainer streams	Distillate rate (kg h <sup>-1</sup> )	0.3	0.447
	Side-stream (F3) mass flow rate (kg h <sup>-1</sup> )	—	130					
EDC3	Pressure (atm)	1	1	Composition	Temperature (°C)	70	70	
	Total stage	60	60		Pressure (atm)	1	1	
	Feed (F3) stage	31	31		DMF (mass fraction)	0.9	0.9	
	Solvent (S3) feed stage	9	7		IL (mass fraction)	0.1	0.1	
	Mass reflux ratio	3.2	9		S1	Total flow rate (kg h <sup>-1</sup> )	6000	6000
	Distillate rate D3 (kg h <sup>-1</sup> )	2.405	2.372		S2	Total flow rate (kg h <sup>-1</sup> )	300	300
					S3	Total flow rate (kg h <sup>-1</sup> )	18	18



**Figure 7. Profiles of composition in the liquid phase along the extractive distillation column (EDC1).**

(■) benzene; (•) thiophene; (▲) DMF.

1 ppm, which can be sold for a high price in chemical markets. The decreased volatilization loss of DMF in the vapor phase can reduce the amount of entrainer required. Thus, only the mixture of DMF and [EMIM][BF<sub>4</sub>] as an entrainer was considered in the subsequent study.

#### Design and simulation of the improved extractive distillation process

The conventional extractive distillation process is shown in Figure 6a and consisted of three extractive distillation columns (i.e., EDC1, EDC2, and EDC3) and three solvent recovery columns (i.e., SRC1, SRC2, and SRC3), which were arranged to ensure that the content of thiophene in the benzene product was less than 1 ppm and the content of thiophene product was 90 wt %. In the conventional process, the feed (benzene and thiophene mixture) entered into EDC1 at the middle stage, whereas the entrainer was introduced at the top. Then, the benzene product (stream D1) was produced at the top of EDC1. At the bottom of the stream containing the entrainer, benzene and thiophene were introduced into the SRC1 to recover the

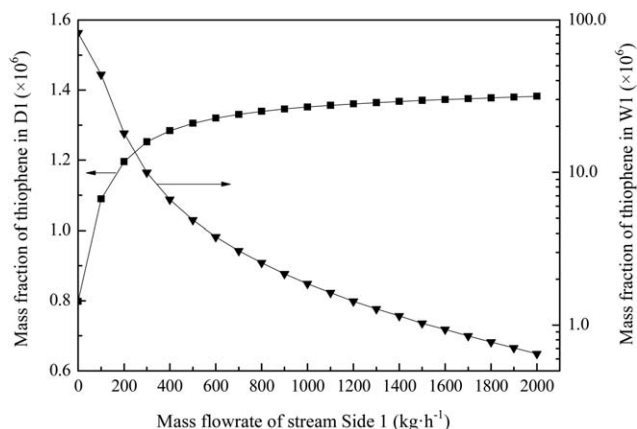


**Figure 8. Effect of mass flow rate of the side-draw stream on the purity of the top and bottom products of EDC1 (constant reflux ratio 6.3).**

(■) mass fraction of thiophene in D1; (▼) mass fraction of thiophene in W1.

entrainer, and at the bottom, the recovered entrainer (stream W1) was obtained and then recycled back to the top of EDC1 after being cooled. The benzene and thiophene mixture obtained at the top of SRC1 entered into EDC2. Then, the benzene stream containing thiophene (stream D2) produced at the top of EDC2 was looped back to F1. The stream at the bottom of EDC2 was introduced into SRC2 to remove the benzene and thiophene mixture from the entrainer. The entrainer was obtained at the bottom of SRC2 (stream W2) and then recycled back to the top of EDC2 after being cooled. The benzene and thiophene mixture obtained at the top of SRC2 entered into EDC3 for further separation. Then, the benzene stream (stream D3) produced at the top of EDC3 was looped back to F2. The entrainer stream at the bottom was introduced into SRC3 to remove small amounts of benzene and thiophene from the entrainer. At the bottom of SRC3, the entrainer (stream W3) was obtained and then recycled back to the top of EDC3 after being cooled. In this process, thiophene was concentrated step by step. At the top of SRC3, the thiophene product (stream D4) containing a small amount of benzene was obtained.

Evidently, the conventional extractive distillation process with six columns (i.e., three extractive distillation columns and three solvent recovery columns) is tedious and should be simplified to decrease equipment investment and energy consumption. As illustrated in Figure 6b, an EDC and an SRC can be combined into an EDC with a side-draw because of the

**Table 3. Comparison of Simulated Stream Results for Conventional and Improved Extractive Distillation Processes**

Streams	Composition (mass fraction)	Conventional process	Improved process
D1	Benzene	1.000	1.000
	Thiophene	145 ppb	160 ppb
	DMF	15 ppb	11 ppb
	IL	trace	trace
D2	Benzene	1.000	1.000
	Thiophene	74 ppm	119 ppm
	DMF	4 ppm	8 ppm
	IL	trace	trace
D3	Benzene	0.997	0.999
	Thiophene	0.003	788 ppm
	DMF	12 ppm	37 ppm
	IL	trace	trace
D4	Benzene	0.099	0.078
	Thiophene	0.901	0.901
	DMF	trace	0.021
	IL	trace	trace
W1	Benzene	trace	21 ppm
	Thiophene	17 ppb	679 ppb
	DMF	0.900	0.880
	IL	0.100	0.120
W2	Benzene	108 ppb	2 ppb
	Thiophene	311 ppm	142 ppb
	DMF	0.900	0.943
	IL	0.100	0.057
W3	Benzene	0.002	457 ppb
	Thiophene	0.021	411 ppm
	DMF	0.881	0.946
	IL	0.097	0.053
Side 1	Benzene	—	0.029
	Thiophene	—	281 ppm
	DMF	—	0.924
	IL	—	0.047
Side 2	Benzene	—	0.021
	Thiophene	—	0.004
	DMF	—	0.930
	IL	—	0.045



**Table 4. Comparison of Heat Duty for Conventional and Improved Extractive Distillation Processes**

Contents	Columns	Heat Duty (kW)	
		Conventional process	Improved process
Condenser	EDC1	−686.77	−759.60
	EDC2	−21.69	−56.27
	EDC3	−1.15	−2.98
	SRC1	−162.60	—
	SRC2	−5.73	—
	SRC3	−0.44	−3.20
	<b>Total</b>	−878.37	−822.06
Reboiler	EDC1	1008.91	1060.25
	EDC2	36.31	78.06
	EDC3	2.02	4.33
	SRC1	171.21	—
	SRC2	6.20	—
	SRC3	0.48	3.25
	<b>Total</b>	1225.13	1145.89

thermal coupling principle.<sup>63</sup> Thus, an improved extractive distillation process with a side-draw was proposed, as shown in Figure 6c. Compared with the conventional process, the original two solvent recovery columns (SRC1 and SRC2 in Figure 6a) were removed in the improved process.

In the process simulation, the feeding mixture was composed of 99.95 wt % benzene and 0.05 wt % thiophene (within the range of the actual compositions) with a flow rate of 1000 kg h<sup>−1</sup> and 90 wt % DMF + 10 wt % [EMIM][BF<sub>4</sub>] as the entrainer. The optimized specifications of the conventional process were determined using the Design Specs module and sensitivity analysis in Aspen Plus with the following constraints: (1) mass fraction of thiophene in streams D1 (benzene product at the top of EDC1) and W1 less than 1 ppm; (2) mass fraction of thiophene in stream D2 less than that in stream F1; (3) mass fraction of thiophene in stream D3 less than that in stream F2; (4) mass purity of thiophene in stream D4 > 90%; and (5) mass fraction of thiophene in stream W2 less than 500 ppm. However, for the improved process, the mass fraction of thiophene in stream W2 should be less than 1 ppm because part of stream W2 will be recycled to EDC1 and mixed with stream S1. The other constraints were the same as in the conventional process. The operating conditions and optimized specifications are given in Table 2.

It is important to determine the location and flow rate of the side-draw streams in the improved process. The composition profile along EDC1 is shown in Figure 7. As seen at stage 56 (numbered from the top to the bottom), the mass fraction of thiophene achieved the maximum value. Thus, stage 56 is the optimum location of the side-draw stream (Side 1). The flow rate of the side-draw stream significantly affected the purity of products at the top and bottom of EDC, as shown in Figure 8. As the flow rate of the side-draw stream was increased, the mass fraction of thiophene in the bottom product W1 decreased but its mass fraction in the top product D1 increased. A large reflux ratio was needed to ensure the benzene product purity (mass fraction of thiophene in stream D1 less than 1 ppm) upon increased side-draw stream flow rate, which indicated that the energy consumption would be high. As a result, the mass flow rate of Side 1 was optimized at 1700 kg h<sup>−1</sup> and the reflux ratio was 6.3 to balance the product purity and energy consumption.

A comparison of the simulation results for the conventional and improved processes is given in Tables 3 and 4. When

compared with the conventional process, the total heat duties of reboilers and condensers decreased by 6.47% and 6.41%, respectively. Therefore, the improved process is more promising for decreasing both energy consumption and equipment investment.

## Conclusions

In this study, the separation of benzene and trace thiophene by extractive distillation was intensified using the DMF and IL mixture as an entrainer instead of a pure organic solvent or IL and by adopting the improved four-column extractive distillation process instead of the conventional six-column process. For a better understanding of the process intensification strategy proposed in this work, VLE data of benzene + thiophene + DMF ternary and benzene + thiophene + DMF + [EMIM][BF<sub>4</sub>] quaternary systems were measured at 101.3 kPa, and the experimental data were correlated with the UNIFAC model for ILs. The results showed that the relative volatility of benzene to thiophene does not obviously increase with the addition of IL to DMF; however, the content of DMF in the vapor phase can be significantly reduced. Thus, the volatilization loss of DMF was greatly decreased. However, the price of IL is higher than that of DMF, and, thus, an economic evaluation of new mixed entrainer should be conducted in future studies.

Furthermore, the conventional extractive distillation process with three extractive distillation columns and three solvent recovery columns was simplified to only four columns. In principle, one extractive distillation column and one solvent recovery column can be combined into one extractive distillation column with a side-draw. The simulation results showed that in comparison with the conventional process, the total heat duties of reboilers and condensers was decreased by 6.47% and 6.41%, respectively, provided that the same purities of benzene and thiophene products were utilized.

It is worth noting that the process intensification strategy presented in this work may be directly extended to trace component separation of other systems, for example, the separation of sulfur-containing compounds and light oil because their separation mechanisms are consistent. Hydrogen bonding driven by electrostatic interactions between IL and sulfur compounds makes ILs effective as green alternative solvents for deep desulfurization.

## Acknowledgment

This work was financially supported by the National Natural Science Foundation of China under grants (Nos. 21476009, 21406007, and U1462104).

## Literature Cited

- Knapp JP, Doherty MF. Minimum entrainer feed flows for extractive distillation: a bifurcation theoretic approach. *AIChE J.* 1994;40:243–268.
- Rodríguez-Donis I, Papp K, Gerbaud V, Joulia X, Rev E, Lelkes Z. Column configurations of continuous heterogeneous extractive distillation. *AIChE J.* 2007;53:1982–1993.
- Shen W, Benyounes H, Gerbaud V. Extension of thermodynamic insights on batch extractive distillation to continuous operation. 1. Azeotropic mixtures with a heavy entrainer. *Ind Eng Chem Res.* 2013;52:4606–4622.
- Shen W, Gerbaud V. Extension of thermodynamic insights on batch extractive distillation to continuous operation. 2. Azeotropic mixtures with a light entrainer. *Ind Eng Chem Res.* 2013;52:4623–4637.
- Benyounes H, Shen W, Gerbaud V. Entropy flow and energy efficiency analysis of extractive distillation with a heavy entrainer. *Ind Eng Chem Res.* 2014;53:4778–4791.

6. Shen W, Benyounes H, Gerbaud V. Extractive distillation: recent advances in operation strategies. *Rev Chem Eng*. 2015;31:13–16.
7. You X, Rodriguez-Donis I, Gerbaud V. Improved design and efficiency of the extractive distillation process for acetone-methanol with water. *Ind Eng Chem Res*. 2015;54:491–501.
8. Naeem M, Al-Rabiah AA, Mughees W. Process simulation of 1-butene and n-butane separation by extractive distillation. *Int J Eng Res Technol*. 2014;3:747–750.
9. Long NVD, Lee M. Optimal retrofit design of extractive distillation to energy efficient thermally coupled distillation scheme. *AIChE J*. 2013;59:1175–1182.
10. Lei Z, Li C, Chen B. Extractive distillation: a review. *Sep Purif Rev*. 2003;32:121–213.
11. Chen B, Lei Z, Li J. Separation on aromatics and nonaromatics by extractive distillation with NMP. *J Chem Eng Jpn*. 2003;36:20–24.
12. Berg L. Separation of benzene and toluene from close boiling nonaromatics by extractive distillation. *AIChE J*. 1983;29:961–966.
13. Matsuda H, Takahara H, Fujino S, Constantinescu D, Kurihara K, Tochigi K, Ochi K, Gmehling J. Selection of entrainers for the separation of the binary azeotropic system methanol + dimethyl carbonate by extractive distillation. *Fluid Phase Equilib*. 2011;310:166–181.
14. Momoh SO. Assessing the accuracy of selectivity as a basis for solvent screening in extractive distillation process. *Sep Sci Technol*. 1991;26:729–742.
15. Lei Z, Wang H, Zhou R, Duan Z. Influence of salt added to solvent on extractive distillation. *Chem Eng J*. 2002;87:149–156.
16. Lei Z, Wang H, Zhou R, Duan Z. Process improvement on separating C4 by extractive distillation. *Chem Eng J*. 2002;87:379–386.
17. Lei Z, Xi X, Dai C, Zhu J, Chen B. Extractive distillation with the mixture of ionic liquid and solid inorganic salt as entrainers. *AIChE J*. 2014;60:2994–3004.
18. Gil ID, Uyazan AM, Aguilar JL, Rodriguez G, Caicedo LA. Separation of ethanol and water by extractive distillation with salt and solvent as entrainer: process simulation. *Braz J Chem Eng*. 2008;25:207–215.
19. Lei Z, Zhou R, Duan Z. Separating 1-butene and 1, 3-butadiene with DMF and DMF with salt by extractive distillation. *J Chem Eng Jpn*. 2002;35:211–216.
20. Lei Z, Wang H, Zhou R, Duan Z. Solvent improvement for separating C4 with ACN. *Comput Chem Eng*. 2002;26:1213–1221.
21. Ligerio EL, Ravagnani TMK. Dehydration of ethanol with salt extractive distillation—a comparative analysis between processes with salt recovery. *Chem Eng Process*. 2003;42:543–552.
22. Ravagnani MASS, Reis MHM, Filho RM, Wolf-Maciel MR. Anhydrous ethanol production by extractive distillation: a solvent case study. *Process Saf Environ Prot*. 2010;88:67–73.
23. Fu J. Salt-containing model for simulation salt-containing extractive distillation. *AIChE J*. 1996; 42:3364–3372.
24. Lei Z, Dai C, Zhu J, Chen B. Extractive distillation with ionic liquids: a review. *AIChE J*. 2014;60:3312–3329.
25. Beste Y, Eggersmann M, Schoenmakers H. Extractive distillation with ionic liquids. *Chem Ing Technol*. 2005;77:1800–1808.
26. Jongmans MTG, Schuur B, de Haan AB. Ionic liquid screening for ethylbenzene/styrene separation by extractive distillation. *Ind Eng Chem Res*. 2011;50:10800–10810.
27. Dai C, Lei Z, Xi X, Zhu J, Chen B. Extractive distillation with a mixture of organic solvent and ionic liquid as entrainer. *Ind Eng Chem Res*. 2014;53:15786–15791.
28. Gutiérrez JP, Meindersma GW, de Haan AB. COSMO-RS-based ionic-liquid selection for extractive distillation processes. *Ind Eng Chem Res*. 2012;51:11518–11529.
29. Martínez AA, Saucedo-Luna J, Segovia-Hernández JG, Hernández S, Gomez-Castro FI, Castro-Montoya AJ. Dehydration of bioethanol by hybrid process liquid-liquid extraction/extractive distillation. *Ind Eng Chem Res*. 2012;51:5847–5855.
30. Orchillés AV, Miguel PJ, Vercher E, Martínez-Andreu A. Ionic liquids as entrainers in extractive distillation: isobaric vapor-liquid equilibria for acetone + methanol + 1-ethyl-3-methylimidazolium trifluoromethanesulfonate. *J Chem Eng Data*. 2007;52:141–147.
31. Ramírez-Márquez C, Segovia-Hernández JG, Hernández S, Errico M, Rong B. Dynamic behavior of alternative separation processes for ethanol dehydration by extractive distillation. *Ind Eng Chem Res*. 2013;52:17554–17561.
32. Orchillés AV, Miguel PJ, Llopis FJ, Vercher E, Martínez-Andreu A. Isobaric vapor-liquid equilibria for the extractive distillation of ethanol + water mixtures using 1-ethyl-3-methylimidazolium dicyanamide. *J Chem Eng Data*. 2011;56:4875–4880.
33. Orchillés AV, Miguel PJ, González-Alfaro V, Vercher E, Martínez-Andreu A. 1-ethyl-3-methylimidazolium dicyanamide as a very efficient entrainer for the extractive distillation of the acetone + methanol system. *J Chem Eng Data*. 2012;57:394–399.
34. Orchillés AV, Miguel PJ, Vercher E, Martínez-Andreu A. Using 1-ethyl-3-methylimidazolium trifluoromethanesulfonate as an entrainer for the extractive distillation of ethanol + water mixtures. *J Chem Eng Data*. 2010;55:1669–1674.
35. Li Q, Zhang J, Lei Z, Zhu J, Huang X. Selection of ionic liquids as entrainers for the separation of ethyl acetate and ethanol. *Ind Eng Chem Res*. 2009;48:9006–9012.
36. Li Q, Xing F, Lei Z, Wang B, Chang Q. Isobaric vapor-liquid equilibrium for isopropanol + water + 1-ethyl-3-methylimidazolium tetrafluoroborate. *J Chem Eng Data*. 2008;53:275–279.
37. Li Q, Zhang J, Lei Z, Zhu J, Xing F. Isobaric vapor-liquid equilibrium for ethyl acetate + ethanol + 1-ethyl-3-methylimidazolium tetrafluoroborate. *J Chem Eng Data*. 2009;54:193–197.
38. Santiago RS, Santos GR, Aznar M. Liquid-liquid equilibrium in ternary ionic liquid systems by UNIFAC: new volume, surface area and interaction parameters. Part I. *Fluid Phase Equilib*. 2010;295:93–97.
39. Santiago RS, Aznar M. Liquid-liquid equilibrium in ternary ionic liquid systems by UNIFAC: new volume, surface area and interaction parameters. Part II. *Fluid Phase Equilib*. 2011;303:111–114.
40. Alevizou EI, Pappa GD, Voutsas EC. Prediction of phase equilibrium in mixtures containing ionic liquids using UNIFAC. *Fluid Phase Equilib*. 2009;284:99–105.
41. Nebig S, Bolts R, Gmehling J. Measurement of vapor-liquid equilibria (VLE) and excess enthalpies (HE) of binary systems with 1-alkyl-3-methylimidazolium bis(trifluoromethylsulfonyl)imide and prediction of these properties and  $\gamma_\infty$  using modified UNIFAC (Dortmund). *Fluid Phase Equilib*. 2007;258:168–178.
42. Nebig S, Gmehling J. Measurements of different thermodynamic properties of systems containing ionic liquids and correlation of these properties using modified UNIFAC (Dortmund). *Fluid Phase Equilib*. 2010;294:206–212.
43. Nebig S, Liebert V, Gmehling J. Measurement and prediction of activity coefficients at infinite dilution ( $\gamma_\infty$ ), vapor-liquid equilibria (VLE) and excess enthalpies (HE) of binary systems with 1,1-dialkyl-pyrrolidinium bis(trifluoromethylsulfonyl)imide using mod. UNIFAC (Dortmund). *Fluid Phase Equilib*. 2009;277:61–67.
44. Nebig S, Gmehling J. Prediction of phase equilibria and excess properties for systems with ionic liquids using modified UNIFAC: typical results and present status of the modified UNIFAC matrix for ionic liquids. *Fluid Phase Equilib*. 2011;302:220–225.
45. Kato R, Gmehling J. Measurement and correlation of vapor-liquid equilibria of binary systems containing the ionic liquids [EMIM][(CF<sub>3</sub>SO<sub>2</sub>)<sub>2</sub>N], [BMIM][(CF<sub>3</sub>SO<sub>2</sub>)<sub>2</sub>N], [MMIM][(CH<sub>3</sub>)<sub>2</sub>PO<sub>4</sub>] and oxygenated organic compounds respectively water. *Fluid Phase Equilib*. 2005;231:38–43.
46. Kim Y, Choi W, Jang J, Yoo K, Lee C. Solubility measurement and prediction of carbon dioxide in ionic liquids. *Fluid Phase Equilib*. 2005;228–229:439–445.
47. Lei Z, Chen B, Li C, Liu H. Predictive molecular thermodynamic models for liquid solvents, solid salts, polymers, and ionic liquids. *Chem Rev*. 2008;108:1419–1455.
48. Lei Z, Zhang J, Li Q, Chen B. UNIFAC model for ionic liquids. *Ind Eng Chem Res*. 2009;48:2697–2704.
49. Bondi A. *Physical Properties of Molecular Liquids, Crystals and Glasses*. New York: Wiley, 1968.
50. Gmehling J, Rasmussen P, Fredenslund A. Vapor-liquid equilibria by UNIFAC group contribution. 2. Revision and extension. *Ind Eng Chem Process Des Dev*. 1982;21:118–127.
51. Press WH, Flannery BP, Teukolsky SA, Vetterling WT. *Numerical Recipes in FORTRAN: The Art of Scientific Computing*, 2nd ed. Cambridge: Cambridge University Press, 1992.
52. Dong L, Zheng D, Wu X. Working pair selection of compression and absorption hybrid cycles through predicting the activity coefficients of hydrofluorocarbon + ionic liquid systems by the UNIFAC model. *Ind Eng Chem Res*. 2012;51:4741–4747.
53. Sander B, Skjold-Jørgensen S, Rasmussen P. Gas solubility calculations. 1. UNIFAC. *Fluid Phase Equilib*. 1983;11:105–126.
54. Palgunadi J, Kang JE, Nguyen DQ, Kim JH, Min BK, Lee SD, Kim H, Kim HS. Solubility of CO<sub>2</sub> in dialkylimidazolium dialkylphosphate ionic liquids. *Thermochim Acta*. 2009;494:94–98.
55. Kleiber M. An extension to the UNIFAC group assignment for prediction of vapor-liquid equilibria of mixtures containing refrigerants. *Fluid Phase Equilib*. 1995;107:161–188.

56. Lei Z, Dai C, Liu X, Xiao L, Chen B. Extension of the UNIFAC model for ionic liquids. *Ind Eng Chem Res.* 2012;51:12135–12144.
57. Lei Z, Dai C, Wang W, Chen B. UNIFAC model for ionic liquid-CO<sub>2</sub> systems. *AIChE J.* 2014;60:716–729.
58. Lei Z, Dai C, Yang Q, Zhu J, Chen B. UNIFAC model for ionic liquid-CO (H<sub>2</sub>) systems: an experimental and modeling study on gas solubility. *AIChE J.* 2014;60:4222–4231.
59. Dai C, Dong Y, Han J, Lei Z. Separation of benzene and thiophene with a mixture of N-methyl-2-pyrrolidinone (NMP) and ionic liquid as the entrainer. *Fluid Phase Equilib.* 2015;388:142–150.
60. Quijada-Maldonado E, Meindersma GW, de Haan AB. Ionic liquid effects on mass transfer efficiency in extractive distillation of water-ethanol mixtures. *Comput Chem Eng.* 2014;71:210–219.
61. Jongmans MTG, Hermens E, Raijmakers M, Maassen JIW, Schuur B, de Haan AB. Conceptual process design of extractive distillation processes for ethylbenzene/styrene separation. *Chem Eng Res Des.* 2012;90:2086–2100.
62. Figueroa JJ, Lunelli BH, Filho RM, Maciel MRW. Improvements on anhydrous ethanol production by extractive distillation using ionic liquid as solvent. *Procedia Eng.* 2012;42:1016–1026.
63. Ramos WB, Figueiredo MF, Brito RP. Optimization of extractive distillation process with a single column for anhydrous ethanol production. *Comput Aided Chem Eng.* 2014;33:1411–1416.
64. Ferro VR, de Riva J, Sanchez D, Ruiz E, Palomar J. Conceptual design of unit operations to separate aromatic hydrocarbons from naphtha using ionic liquids. COSMO-based process simulations with multi-component “real” mixture feed. *Chem Eng Res Des.* 2015;94:632–647.
65. Ferro VR, Ruiz E, de Riva J, Palomar J. Introducing process simulation in ionic liquids design/selection for separation processes based on operational and economic criteria through the example of their regeneration. *Sep Purif Technol.* 2012;97:195–204.
66. Ruiz E, Ferro VR, de Riva J, Moreno D, Palomar J. Evaluation of ionic liquids as absorbents for ammonia absorption refrigeration cycles using COSMO-based process simulations. *Appl Energy.* 2014;123:281–291.

Manuscript received Apr. 22, 2015, and revision received July 25, 2015.